UNIVERSITÀ DEGLI STUDI FIRENZE

DISIA
DIPARTIMENTO DI STATISTICA, INFORMATICA, APPLICAZIONI "GIUSEPPE PARENTI"

Combining Markov Switching and Smooth Transition in Modeling Volatility: A Fuzzy Regime MEM

Giampiero M. Gallo, Edoardo Otranto

DISIA WORKING PAPER
2016/02

Combining Markov Switching and Smooth Transition in Modeling Volatility: A Fuzzy Regime MEM

Giampiero M. Gallo

Dipartimento di Statistica, Informatica, Applicazioni "G. Parenti", Università di Firenze

Via G. B. Morgagni, 59 - 50134 Firenze, Italy (*gallog@disia.unifi.it*)

Edoardo Otranto

Dipartimento di Economia and CRENoS,

Università di Messina, Piazza Pugliatti, 1 - 98122 Messina, Italy (*eotranto@unime.it*)

Abstract

Volatility in financial markets alternates persistent turmoil and quiet periods. Modelling realized volatility time series requires a specification in which these subperiods are adequately represented. Changes in regimes is a solution, but the question of whether transition between periods is abrupt or smooth remains open. We provide a new class of models with a set of parameters subject to abrupt changes in regime and another set subject to smooth transition changes. These models capture the possibility that regimes may overlap with one another (*fuzzy*). The empirical application is carried out on the volatility of four US indices.

Keywords: Volatility modeling, Volatility forecasting, Multiplicative Error Model, Markov Switching, Smooth Transition

1 Introduction

A recent strand of financial econometrics literature underlines as the profile of the realized volatility of financial time series is subject to frequent changes, which can assume the form of an abrupt change of regime, a smooth transition toward a different regime, an isolated jump, etc. Several recent studies develop models capturing all these features or concentrating on just some of them. For example, Gallo and Otranto (2015) extend the family of Asymmetric Multiplicative Error Models (AMEM) of Engle (2002) and Engle and Gallo (2006) to include Markovian changes in regime (abrupt changes) and smooth transitions to other regimes (gradual changes) with two separate models, called Markov Switching (MS)–AMEM and Smooth Transition (ST)– AMEM respectively. Andersen *et al.* (2007) provide the specification extensions related to jumps by inserting in the HAR model of Corsi (2009) an explicative variable depending on the comparison between the realized volatility and the realized bi-power variation of the time series, whereas Caporin *et al.* (2014b) add, in the same HAR model, a volatility jump term following a compound Poisson process. A similar extension was adopted by Caporin *et al.* (2014a) to include jumps in the MEM.

The correct detection of the several kinds of change is a crucial task in the analysis of the forecasting performance of the models. A typical result is the trade–off existing between the in–sample and out–of–sample performance; in particular, Gallo and Otranto (2015), analyzing the realized kernel volatility (Barndorff-Nielsen *et al.*, 2008) of the S&P500 index with several alternative models belonging to the AMEM and HAR classes, notice a better in–sample fitting of the MS–AMEM and a superior out–of–sample performance of the ST–AMEM. Of course, since they were obtained on just one series, the generalization of these results is one of the goals of this paper. Moreover, it is appealing to seek for a model characterized by good performances in both the in–sample and out–of–sample perspective, giving it an intermediate position between MS–AMEM and ST–AMEM. Our suggestion is to provide a new model which contains both kinds of dynamics, the MS and the ST, involving the possibility to capture both the abrupt and the gradual changes in the series.

This idea is developed by considering the coefficients linked to the level of the volatility subject to discrete changes (represented by different regimes or states) and the coefficients representing the dependence on the past as continuously time–varying, by using a smooth transition function depending on a forcing variable known one period in advance and related to the series analyzed. This specification provides a range of possible values of the local average volatility within each regime which may be overlapping, losing the classical definition of regime linked to well separate states. This is consistent with the realistic cases in which some periods can not be cleared assigned to a certain regime. For this reason we define this class of models the Fuzzy Regime AMEM with n states (FR(n)–AMEM).[1]

We will verify the in–sample and out–of–sample performance of this new class of models applying them to four different realized volatility series and comparing them with

[1]This model has some similarities with the Flexible MS model proposed by Otranto (2015), providing the possibility to have time–varying coefficients within each regime, but not the possibility of overlapping states.

the MS– and ST–AMEMs of Gallo and Otranto (2015) to verify if they are able to capture the better in–sample characteristics of the first and the out–of–sample ones of the latter. Moreover, we will estimate also the *classical* AMEM and HAR as useful benchmarks.

The paper is organized as follows: in the next section we will describe the FR(n)–AMEM, with a particular focus on the simple 2-state case to illustrate the nature of the fuzzy regimes. Section 3 is devoted to the empirical application of the model. We first devote some special attention to the comparison of the information derived from the FR(2) model with those derived from MS(3) and ST models for the S&P500. We then extend the number of models and the number of US realized kernel volatility time series including next to the S&P500, also the Russell 2000, the Dow Jones 30, and the Nasdaq 100. In– and out–of–sample performances are evaluated on the basis of single loss functions and a synthesis thereof to evaluate contemporaneously the in–sample and out–of–sample performance. Some final remarks conclude the paper.

2 Combining Switching Regimes and Smooth Transitions

The Multiplicative Error Model (MEM) has shown to have many desirable properties for the analysis of the realized volatility. Among the reasons that enable its success we cite the direct representation of the levels of volatility without (log) transformations and the possibility to extend it to include asymmetric effects (Engle and Gallo, 2006), Markovian or smooth transition dynamics (Gallo and Otranto, 2015), presence of jumps (Caporin *et al.*, 2014b). The model we propose is a combination of the MS–AMEM and the ST–AMEM proposed by Gallo and Otranto (2015).

Let y_t the realized volatility of a certain index at time t ($t = 1, \dots, T$), μ_{t,s_t} a latent factor representing its conditional mean, s_t a discrete latent variable ranging in $[1, \dots, n]$, representing the regime at time t, ε_t a random disturbance and D_t a dummy variable which is 1 when the return of the index at time t is negative. The MS(n)–AMEM, where n indicates the number of regimes, is given by:

$$\begin{aligned} y_t &= \mu_{t,s_t}\varepsilon_t, \qquad \varepsilon_t|s_t \sim \text{Gamma}(a_{s_t}, 1/a_{s_t}) \text{ for each } t, \\ \mu_{t,s_t} &= \omega + \textstyle\sum_{i=1}^{n} k_i I_{s_t} + \alpha_{s_t} y_{t-1} + \beta_{s_t}\mu_{t-1,s_{t-1}} + \gamma_{s_t} D_{t-1} y_{t-1} \end{aligned} \tag{2.1}$$

The first equation follows the typical MEM structure suggested by Engle (2002), obtained as the product of two positive unobservable factors; as in Engle and Gallo (2006), the Gamma distribution of the disturbances depends only on the scale parameter, which in (2.1) changes with the regime (a_{s_t}), so that its mean is equal to 1 and its variance equal to $1/a_{s_t}$. The second equation represents the dynamics of the mean, which follows a sort of GARCH(1,1)–type dynamics, with the intercept $\omega + \sum_{i=1}^{n} k_i I_{s_t}$ (where I_{s_t} is the indicator of the state; $k_1 = 0$, $k_i >= 0$ for $i > 1$), which increases with the state s_t. The dynamics of the latent state variable s_t is driven by a Markov chain, such that:

$$Pr(s_t = j|s_{t-1} = i, s_{t-2}, \dots) = Pr(s_t = j|s_{t-1} = i) = p_{ij}. \tag{2.2}$$

We hypothesize that the volatility levels increase with the regime s_t.

Gallo and Otranto (2015) define also the ST–AMEM as:

$$\begin{aligned} y_t &= \mu_t \varepsilon_t, \qquad \varepsilon_t \sim \text{Gamma}(a, 1/a) \text{ for each } t \\ \mu_t &= \omega + \alpha_t y_{t-1} + \beta_t \mu_{t-1} + \gamma_t D_{t-1} y_{t-1} \end{aligned} \tag{2.3}$$

The coefficients α_t, β_t, γ_t are smooth transition parameters,[2] which follow a simple linear dynamics depending on a smooth function $0 \leq g_t \leq 1$:

$$\begin{aligned} \alpha_t &= \alpha_0 + \alpha_1 g_t \\ \beta_t &= \beta_0 - \beta_1 g_t \\ \gamma_t &= \gamma_0 + \gamma_1 g_t \\ g_t &= (1 + \exp(-\delta(x_t - c)))^{-1}. \end{aligned} \tag{2.4}$$

where x_t is a forcing variable driving the smooth movements, generally linked to the volatility movements. Imposing the nonnegativity of the coefficients α_0, α_1, β_0, β_1, γ_0, γ_1, the effect on the time-varying coefficients α_t, β_t, γ_t, increasing the smooth function g_t, is an increase of the coefficients α_t and γ_t, expressing the effect of the last volatility level, and a decrease of β_t, which, in turn, contributes to a decrease in the persistence effect. Notice that in (2.3) the coefficient a of the Gamma distribution is not time–varying because the levels of the volatility are assumed not subject to discrete jumps, but to continuous changes; in practice the smooth transition changes of the level of volatility capture also the possible different spread and the model can fit the data with a constant variance.

The FR(n)–AMEM combines the characteristics of models (2.1) and (2.3) and it is defined as:

$$\begin{aligned} y_t &= \mu_{t,s_t} \varepsilon_t, \qquad \varepsilon_t | s_t \sim \text{Gamma}(a, 1/a) \text{ for each } t, \\ \mu_{t,s_t} &= \omega + \textstyle\sum_{i=1}^{n} k_i I_{s_t} + \alpha_t y_{t-1} + \beta_t \mu_{t-1,s_{t-1}} + \gamma_t D_{t-1} y_{t-1} \end{aligned} \tag{2.5}$$

As in the ST–AMEM, the Gamma distribution of the disturbances depends only on the constant parameter a, whereas the second equation represents the new specification of the dynamics of the mean, which is composed by one switching and three smooth transition coefficients. The switching coefficient is the intercept and the coefficients α_t, β_t, γ_t are smooth transition parameters, following the (2.4) specification. In our applications we will consider the lagged VIX (Whaley, 1993) as forcing variable, but other choices are possible.

Models MS(n)–AMEM and ST–AMEM are not nested in model (2.5). In fact for the MS–AMEM we hypothesize that $\alpha_t = \alpha_{s_t}$, $\beta_t = \beta_{s_t}$, $\gamma_t = \gamma_{s_t}$, which do not depend on g_t, so that c and δ are nuisance parameters. The ST–AMEM is not nested in the FR–AMEM because it considers a constant intercept or an intercept depending on g_t. When all the coefficients are constant we obtain the simple AMEM of Engle and Gallo (2006).

The peculiarity of the FR(n)–AMEM is that the n regimes cannot be clearly separated, but the same observation could be assigned to a regime or another one, depending on the value of the smooth transition function g_t. To better understand this characteristic, let

[2] In Gallo and Otranto (2015) γ_t was constant.

us consider the *local average volatility* (LAV hereafter) of the series y_t, conditional on the regime and the value of g_t, under the usual stationarity hypothesis; this indicator corresponds to the unconditional volatility when all the coefficients are constant (as in the AMEM case). For the sake of simplicity let us consider the 2-state case, but the results are easily extended to the general n-state model. Let $u_{t,s_t,g_t} = E(\mu_{s_t,t}|s_t, s_{t-1}, g_t)$ the LAV at time t; it is derived from the second equation of (2.5) and is given by:

$$u_{t,s_t,g_t} = \omega + k_2 I_2 + (\alpha_t + \beta_t + \gamma_t/2) u_{t-1,s_{t-1},g_{t-1}} \tag{2.6}$$

Adding the constraint $(\alpha_1 + \gamma_1/2) \geq \beta_1$, u_{t,s_t,g_t} will not decrease when g_t increases and will not decrease with the regime ($u_{t,2,g_t} \geq u_{t,1,g_t}$ because $k_2 \geq 0$). Also, when $s_t = s_{t-1}$ and $g_t = g_{t-1}$, equation (2.6) can be written in a manner similar to the classical unconditional volatility expression:

$$u_{t,s_t,g_t} = \frac{\omega + k_2 I_2}{1 - \alpha_t - \beta_t - \gamma_t/2} \tag{2.7}$$

This implies that the minimum (maximum) of u_{t,s_t,g_t} is reached in correspondence of both g_t and g_{t-1} equal to 0 (1). As a consequence, we can detect a global minimum and maximum of the LAV and its range for each regime; calling $u^l_{s_t}$ and $u^h_{s_t}$ the lower and higher extremes of the LAV in regime s_t, we have:

$$\begin{aligned}
u^l_1 &= min(u_{t,1,g_t}) = E(\mu_t|s_t = 1, s_{t-1} = 1, g_t = 0) = \tfrac{\omega}{1-\alpha_0-\beta_0-\gamma_0/2} \\
u^h_2 &= max(u_{t,2,g_t}) = E(\mu_t|s_t = 2, s_{t-1} = 2, g_t = 1) = \tfrac{\omega+k_2}{1-\alpha_0-\alpha_1-\beta_0+\beta_1-(\gamma_0+\gamma_1)/2} \\
u^h_1 &= max(u_{t,1,g_t}) = E(\mu_t|s_t = 1, s_{t-1} = 2, g_t = 1) = \omega + (\alpha_0 + \alpha_1 + \beta_0 - \beta_1 + \tfrac{\gamma_0+\gamma_1}{2}) u^h_2 \\
u^l_2 &= min(u_{t,2,g_t}) = E(\mu_t|s_t = 2, s_{t-1} = 1, g_t = 0) = \omega + k_2 + (\alpha_0 + \beta_0 + \tfrac{\gamma_0}{2}) u^l_1
\end{aligned} \tag{2.8}$$

The two ranges of the local average volatilities in different regimes may overlap, providing a sort of fuzzy regime. In practice model (2.5) provides an inference on the regime as each MS model, but the levels of the LAV are not clearly separated among regimes. In other words, if $u^h_1 > u^l_2$, then the set $[u^l_2; u^h_1]$ is the overlapping area and the local average volatilities can be classified (borrowing the set theory terminology, see Zadeh (1965)) in the following way:

- crisp zone 1: local average volatilities ranging in $[u^l_1; u^l_2]$;
- fuzzy zone: local average volatilities ranging in $[u^l_2; u^h_1]$;
- crisp zone 2: local average volatilities ranging in $[u^h_1; u^h_2]$;

In Figure 1 we illustrate a graphical example to better interpret the fuzzy and crisp zones; we consider a simple FR(2)–AMEM with $\beta_t = \gamma_t = 0$); the other coefficients are $\omega = 1$, $k_2 = 3$, $\alpha_0 = 0.5$, $\alpha_1 = 0.4$. The Figure shows the behavior of the LAV in the two regimes in correspondence of g_t. The two curves do not intersect but, in the fuzzy zone (gray area), they can assume the same value in correspondence of two different values of

g_t; in other words a certain level of the unconditional volatility can be reached in state 1 in correspondence of a certain g_t or in state 2 in correspondence of a lower g_t. In practice in the fuzzy zone the assignment of an observation to regime 1 or 2 depends on the value of g_t.

The extension to the $n-$state case is simple; for the state j, the range of the LAV is given by:

$$\begin{aligned} u_j^l &= \omega + \textstyle\sum_{i=1}^{j} k_i + (\alpha_0 + \beta_0 + \gamma_0/2)u_1^l \\ u_j^h &= \omega + \textstyle\sum_{i=1}^{j} k_i + (\alpha_0 + \alpha_1 + \beta_0 - \beta_1 + \gamma_0/2 + \gamma_1/2)u_n^h \end{aligned} \tag{2.9}$$

From (2.9), it is evident that the differences between the lowest (highest) LAV of two states is due exclusively to the changes in the intercept, so it is likely that the fuzzy zones are very large with respect to the crisp zones. This fact could imply some difficulty in the interpretation of regimes when the number of states is more than two, since several regimes will have overlapping areas. What we want to stress is that we gain in terms of flexibility of the model and goodness of fit, as empirically shown in what follows especially by the FR(3)–AMEM. Nonetheless, we can discuss some features of the FR(2)–AMEM model to provide some graphical illustration of the mechanisms behind this new approach.

For reference purposes, let us introduce a corresponding formula for the MS–AMEM, given by:

$$\begin{aligned} u_{t,s_t} &= \omega + \textstyle\sum_{i=1}^{n} k_i I_{s_t} + (\alpha_{s_t} + \beta_{s_t} + \gamma_{s_t}/2)u_{t-1,s_{t-1}} \quad \text{if } s_t \neq s_{t-1} \\ u_{t,s_t} &= \tfrac{\omega + \sum_{i=1}^{n} k_i I_{s_t}}{1-\alpha_{s_t}-\beta_{s_t}-\gamma_{s_t}/2} \qquad\qquad\qquad\qquad \text{if } s_t = s_{t-1} \end{aligned} \tag{2.10}$$

whereas the one for the ST–AMEM is:

$$u_{t,g_t} = \omega + (\alpha_t + \beta_t + \gamma_t/2)u_{t-1,g_{t-1}} \tag{2.11}$$

We can use the strong relationship between the regime and g_t to assign the observations to a crisp or a fuzzy zone. Let us consider again the two-state case (the extension to a generic $n-$state case is trivial but notationally cumbersome); the conditional mean (second equation of (2.5) is:

$$\mu_{s_t,t} = \omega + k_2 I(s_t) + \alpha_0 y_{t-1} + \beta_0 \mu_{s_{t-1},t-1} + \gamma_0 D_{t-1} y_{t-1} + g_t(\alpha_1 y_{t-1} - \beta_1 \mu_{s_{t-1},t-1} + \gamma_1 D_{t-1} y_{t-1})$$

If the observation at time t falls in a fuzzy zone, then there will exist a value of g_t (call it g_t^*) such that:

$$g_t^* = \frac{\mu_{s_t,t} - \omega - k_2(1 - I_{s_t}) - \alpha_0 y_{t-1} - \beta_0 \mu_{s_{t-1},t-1} - \gamma_0 D_{t-1} y_{t-1}}{\alpha_1 y_{t-1} - \beta_1 \mu_{s_{t-1},t-1} + \gamma_1 D_{t-1} y_{t-1}}$$

and $0 \leq g_t^* \leq 1$.

If $g_t^* < 0$ or $g_t^* > 1$, it is a not admissible value and the observation at time t falls in a crisp zone.

3 Empirical Analysis

3.1 The Data and the Models

We apply the FR(n)–AMEM, with $n = 2$ and 3, to four realized kernel volatility series of the main indices of the US markets: S&P500, Russell 2000, Dow Jones 30, Nasdaq 100. The forcing variable adopted for the smooth transition function is the lagged VIX. The realized kernel volatility is an estimator of the integrated volatility of a diffusion process, proposed by Barndorff-Nielsen *et al.* (2008), possessing the important property of robustness to market microstructure noise. The data relative to the series analyzed in this work are taken from the Oxford-Man Institute Realized Library version 0.2 (Heber *et al.*, 2009), and are annualized, i.e. we consider the square root of the realized kernel variance multiplied by $100\sqrt{252}$. We cover the period 2 January 2004–5 May 2015 with daily observations, using the data until 31 December 2013 for the in–sample evaluation and the rest for the out–of–sample case. In Figure 2 the four series are depicted. They show similar behavior with common highest peaks, in particular the bursts of volatility starting in September 2008. The out–of–sample period is characterized by frequent movements with no high peaks.

In addition to the FR(2)–AMEM and the FR(3)–AMEM we have estimated a MS(3)–AMEM and a ST–AMEM, following the specification given in Gallo and Otranto (2015). Moreover, we have considered two simple benchmark models as AMEM and HAR:

- **AMEM**:

$$y_t = \mu_t \varepsilon_t, \qquad \varepsilon_t \sim \text{Gamma}(a, 1/a) \text{ for each } t,$$

$$\mu_t = \omega + \alpha y_{t-1} + \beta \mu_{t-1} + \gamma D_{t-1} y_{t-1},$$

- **HAR**:

$$y_t = \mu_t \varepsilon_t, \qquad \varepsilon_t \sim \text{Gamma}(a, 1/a) \text{ for each } t$$

$$\mu_t = \omega + \alpha_D y_{t-1} + \alpha_W \bar{y}_{t-1}^{(5)} + \alpha_M \bar{y}_{t-1}^{(22)},$$

  where the three independent variables of the second equation express past volatilities aggregated at daily, weekly and monthly frequency respectively.

In Table 2 we show the estimation results for the four indices using the FR(3)–AMEM, that, as we will see, shows in general the best performance. All the indices are characterized from a strong persistence in state 2 and the probability to switch to state 1 at time t, when $s_{t-1} = 3$, near to 1. For the Russell index we set the parameters p_{12}, p_{21} and α_0 equal to zero to get convergence.

In Table 3 we show the extreme values of the LAV for the ST, FR(2) and FR(3) models and the LAV of each state of MS(3) (expressed by the second equation in (2.10), which is the most frequent case, as showed in the first panel of Figure 3). It is interesting to notice as the highest values of the ST–AMEM are very low if compared to the highest peaks of the realized volatility. Also the presence of a third regime in the FR model provides the possibility to identify very high peaks, excluding the Russell case, where the maximum value of the LAV in the third regime is equal to the LAV of the third regime of the static

MS(3) model. Of course these extreme values are theoretical, depending, in practice, on the value of g_t in the sample adopted.

3.2 Interpretation of Fuzzy Regimes

In order to gain deeper insights on the features of the FR–AMEM (in particular for the interpretation of the regimes), contrasting its results with those derived from a suitable MS–AMEM and a ST–AMEM. For the sake of illustration, we keep on considering a 2-state FR model, with two crisp and one fuzzy zone; the natural comparison is made in terms of a 3-state MS model, because the fuzzy zone of a FR(2)–AMEM could be considered as an alternative to the second regime of a MS(3)–AMEM. In what follows, the inference on the Markovian regimes is obtained from the smoothed probabilities in each model, calculated over the full span, assigning the time t to the regime with the highest smoothed probability at that time.

In Figure 3 we show the time series profile of the local average volatilities derived for the three models, starting from the MS(3)–AMEM (expression (2.10) in the top panel), then the ST–AMEM (expression (2.11) in the middle panel) and then the FR(2)–AMEM (expression (2.6 in the bottom panel). In all three panels we overlap the values of the local average volatilities to the realized volatility series. For all models, we confirm the difficulty highlighted by Gallo and Otranto (2015) to capture the burst of volatility of October 2008. For the MS(3)–AMEM, it is clear that its LAV is subject to abrupt and discrete changes, (usually between three constant levels): while, on the one hand, this allows for a clear identification of which regime each observation is attributed to, on the other, it presents the inconvenient feature that fairly different values of realized volatility are associated with the same level of LAV. This is apparent from the first period in which we have a prolonged constant level of LAV, but it is even more striking for the third regime, where the LAV is often very high relative to the corresponding observed volatility value. The ST–AMEM and FR(2)–AMEM show a similar dynamics of local average volatilities relative to one another, but the latter better follows the profile of the realized volatility, especially for its highest values (the maximum level of the LAV in the ST model is equal to 32.3 points versus a maximum of 41.7 in the FR case). In practice, the FR model has the same desirable features as the ST model in terms of flexibility, but exploits the MS properties to better identify the frequent jumps and abrupt changes.

In Figure 4 we reconstruct the distributions of the realized kernel volatilities for the MS and the FR models, highlighting the regimes identified on the basis of the inference on the states. The different attribution of observations to regimes across models is more evident for lower values, while the highest values are uniformly assigned to the highest regime. In reference to the characterization of fuzzy regimes, we can notice that they are typical for volatility values under 40%. Looking at Table 1, the average value of the volatility when the observation falls in regime 2, but in a fuzzy zone, is lower than the average of the fuzzy zone in regime 1; this result is coherent with Figure 1, where we saw that the grey area is common to the lowest values of regime 2 and the highest values of regime 1. From the same table, let us notice that the regime 2–crisp within the FR model captures just the highest peaks: on average, this regime includes fewer observations and has a higher average value (by more than 12%) than the third regime within the MS model.

By and large, the regime 2–fuzzy in the FR model matches the highest peaks of regime 1 in the MS(3) model, whereas observations in the regime 1–fuzzy fall into the second regime of MS(3). This regularity is confirmed by comparing Figure 5, where we show the inference about the regimes within the FR(2) model, with the first graph of Figure 3, where derive the inference about the regimes within the MS(3) model.

In Figure 5 we distinguish between fuzzy (dotted blue) and crisp (black continuous) classification within either regime. Notice that the volatility values belonging to the regime 1–crisp are very small, isolating the periods of very low volatility, whereas the regime 2–crisp corresponds only to the highest episodes. The observations in the fuzzy area are obviously in–between cases: we can notice that the regime 1–fuzzy generally captures cases in which there is a smooth reduction in volatility whereas regime 2–fuzzy generally corresponds to a smooth increase in volatility. Typically we reach regime 2–crisp by passing through regime 2–fuzzy (a burst from a volatility already increasing), while the downward evolution from regime 2–crisp is characterized by a change to regime 1 entering its fuzzy zone. For ease of reference, we report in Table 4 the reconstruction of turbulences occurring in the US and European markets which characterize the dates assigned to regime 2–crisp. Reassuringly, we find all major related events, from Bear Sterns, to Lehman Brothers to the US Budget crisis and the evolution of the Greek debt crisis with the inception of uncertainty about the solidity of the Euro institutional arrangements.

3.3 Comments on Other Models and Other Indices

The inference on the regime is quite similar across the four indices. In Table 5 we show a classification of the dates, indicating the percentage of cases where a) the volatilities of the four indices at time t are all assigned to the same state, b) just three indices to the same state, c) two indices to the same state and two to another one (but the same), d) two indices to one state and the other two to two other separate states,[3] using FR(3)–AMEM, FR(2)–AMEM and MS(3)–AMEM. For a large part of the observations we assign three or four indices contemporaneously to the same state (cases a) and b)): in particular, more than 88% using the MS(3)–AMEM, more than 81% using FR(2)–AMEM and more than 94% using FR(3)–AMEM. The latter shows more than 61% of agreement of the indices within the same regime (case a)).

The comparison among the six models (HAR, AMEM, ST–AMEM, MS(3)–AMEM, FR(2)–AMEM, FR(3)–AMEM) is conducted in terms of residual autocorrelation and Mean Squared Errors (MSE) and Mean Absolute Errors (MAE) both for the in–sample and out–of–sample cases. In Table 6 we show the p-values of the Ljung–Box statistics for each model and each index in correspondence of several lags. It is evident the presence of residual correlation in the HAR model (a result coherent with (Gallo and Otranto, 2015)), whereas the MEM family seems able to satisfy the hypothesis of uncorrelatedness, with some exceptions. In particular we notice a disappointing performance of the MS(3)–AMEM for the Russell 2000 and a general improvement of the test statistics for the FR model passing from 2 to 3 regimes.

We find interesting the models performance in terms of fitting and forecasting. As

[3] In the FR(2)–AMEM, the last case is not possible.

in Gallo and Otranto (2015), we have considered 1 and 10 steps ahead out–of–sample forecasts, evaluating 336 observations corresponding to the most recent period (2014 and some of 2015). For the out–of–sample forecasts we have used the model estimated in–sample, fixing the estimated parameters for the full out–of–sample period. In Table 7 we show the loss functions for each index: in general, we confirm the result that the MS(3)–AMEM performs better than ST–AMEM in–sample and the opposite is true out–of–sample. One interesting feature of the FR models is their nature of striking a compromise between the two, as they reach a satisfactory performance across in– and out–of–sample, since they are almost always the best or the second best model.

To decide what model performs globally better in in– and out–of–sample terms, it is convenient to evaluate the indices in relative terms, considering their relative performance with respect to the HAR model adopted as a benchmark model. Each relative variation of the loss function l of model M is given by:

$$v_M = \frac{l_M - l_{HAR}}{l_{HAR}},$$

with generally an expected negative sign (an improvement relative to HAR). To synthesize results, a global loss function G_M for model M may be derived as weighted average of the resulting six loss functions (MSE and MAE, in– and 1– and 10–steps ahead out–of–sample):

$$G_M = \sum_l w_l v_M, \qquad \sum_l w_l = 1 \tag{3.1}$$

We consider four possible global loss functions, differing by the set of weights used. We choose

1. *uniform*: each w_l equal to $1/6$;
2. *oos oriented*: the weights of the in–sample loss functions equal to 0.1 and the weights of the out–of–sample loss functions equal to 0.2;
3. *oos short term (st) oriented*: the weights of the 1–step ahead out–of–sample loss functions equal to 0.3 and the others equal to 0.1;
4. *oos long term (lt) oriented*: the weights of the 10–step ahead out–of–sample loss functions equal to 0.3 and the others equal to 0.1.

The performance in terms of global functions is better, the more G_M decreases away from the value $G_M = 0$ (which marks the same performance as the HAR model).

In Table 8 we show the evaluation derived from the four alternative global loss functions (3.1). For the S&P500 index we notice a better behavior of the FR models considering the uniform loss function; when the out–of–sample performance has more importance in the evaluation, the good behavior of the ST–AMEM predominates, but FR(2)–AMEM wins in the short term horizon; also FR(3)–AMEM is always the second best (the best in the uniform case). For the Russell index the MS(3)–AMEM seems to have the best performance, but, recalling the results in Table 6, it suffers from a clear presence of autocorrelation in its residuals; again FR(3)–AMEM is always the second best and outperforms

MS(3)–AMEM in the short term forecasting. The DJ and Nasdaq indices clearly favor the FR(3)–AMEM, which is the best model with respect to all the global loss functions, excluding the long term forecasting case of DJ, where it closely loses to ST–AMEM (with a difference, which is less than 0.002).

4 Conclusions

The existence of waves of turbulence ensuing from events affecting the national and global economies, has characterized the behavior of volatility in financial markets, posing a serious challenge to econometric modeling of the corresponding time series. The main feature that one can notice in the corresponding graphs is that the average level of volatility changes through time at low frequencies, with short term dynamics around such levels marked by slow mean reversion (persistence).

In this paper, we have elaborated on a large stream of literature that extends the study of volatility in a GARCH framework, by introducing Markov switching features to the specification for the return conditional variance and, alternatively, Smooth Transition across different average levels; see, for example, Maheu and McCurdy (2002), Maheu and McCurdy (2007), Maheu and McCurdy (2011), McAleer and Medeiros (2008). In particular we have concentrated on Multiplicative Error Models and their MS and ST extensions studied by Gallo and Otranto (2015) by introducing a new class of models that combines features of both. The specification allows for a characterization of the observations in which while maintaining assignment to regimes, within each regime we identify observations belonging to a sharp characterization of the regime (called *crisp*) and observations assigned to another range, called *fuzzy*, seen as a sort of intermediate case between regimes. From the empirical results, and for the case of two regimes, we interpret the regime 1–crisp as a regime of low volatility, the regime 2–crisp as a regime corresponding to major turmoil events. The fuzzy regimes are characterized by a slow increase in volatility (and hence a slow transition from low to high volatility, regime 1–fuzzy), respectively, by a slow decrease in volatility (and hence a slow transition from high to low volatility, regime 2–fuzzy).

The analysis was carried out on four major US indices which represent various degrees of market depth, capitalization and liquidity: we chose to specify models for the realized kernel volatility measures which can be seen as the best available realized measures of volatility (with robustness to jumps and market microstructure noise). We had several variants of the suggested models estimated, changing the number of regimes considered in the MS component, and keeping the Corsi (2009) HAR as a benchmark reference as in other studies. The estimation results were evaluated both in– and out–of–sample with a number of loss functions, then conveniently summarized in relative terms with respect to the benchmark and then aggregated in a global loss function with alternative choices of weights to adhere to different goals a model could be geared to. The general result is that the introduction of the fuzzy area allows for a convenient tradeoff between in–sample performance where MS models perform the best and out–of–sample, where the ST model comes out first, in line with Hansen and Timmerman (2015).

The fuzzy regime models also seem to capture the explosion in volatility following the

bankruptcy of Lehman Brothers in Sep.–Oct. 2008, in the two regime case, we are capable of interpreting each observation assigned to the regime 2–crisp in terms of major events which affected the US markets with the evolution of the subprime mortgage crisis in 2008 and then the US Budget and the uncertainty surrounding the Euro Area institutional arrangements in 2011.

References

Andersen, T. G., Bollerslev, T., and Diebold, F. X. (2007). Roughing it up: Including jump components in the measurement, modeling and forecasting of return volatility. *Review of Economics and Statistics*, **89**, 701–720.

Barndorff-Nielsen, O. E., Hansen, P. R., Lunde, A., and Shephard, N. (2008). Designing realised kernels to measure the ex-post variation of equity prices in the presence of noise. *Econometrica*, **76**, 1481–1536.

Caporin, M., Rossi, E., and Santucci De Magistris, P. (2014a). Chasing volatility: a persistent multiplicative error model with jumps. Technical report.

Caporin, M., Rossi, E., and Santucci De Magistris, P. (2014b). Volatility jumps and their economic determinants. *Journal of Financial Econometrics*, **forthcoming**.

Corsi, F. (2009). A simple approximate long-memory model of realized volatility. *Journal of Financial Econometrics*, **7**, 174–196.

Engle, R. F. (2002). New frontiers for ARCH models. *Journal of Applied Econometrics*, **17**, 425–446.

Engle, R. F. and Gallo, G. M. (2006). A multiple indicators model for volatility using intra-daily data. *Journal of Econometrics*, **131**, 3–27.

Gallo, G. M. and Otranto, E. (2015). Forecasting realized volatility with changing average volatility levels. *International Journal of Forecasting*, **31**, 620–634.

Hansen, P. R. and Timmerman, A. (2015). Discussion of "comparing predictive accuracy, twenty years later" by francis x. diebold. *Journal of Business and Economic Statistics*, **33**, 17–21.

Heber, G., Lunde, A., Shephard, N., and Sheppard, K. (2009). Omi's realised library, version 0.1. Technical report, Oxford-Man Institute, University of Oxford.

Maheu, J. M. and McCurdy, T. H. (2002). Nonlinear features of realized fx volatility. *Review of Economics and Statistics*, **84**(4), 668–681.

Maheu, J. M. and McCurdy, T. H. (2007). Components of market risk and return. *Journal of Financial Econometrics*, **5**(4), 560–590.

Maheu, J. M. and McCurdy, T. H. (2011). Do high-frequency measures of volatility improve forecasts of return distributions? *Journal of Econometrics*, **160**, 69–76.

McAleer, M. and Medeiros, M. (2008). A multiple regime smooth transition heterogeneous autoregressive model for long memory and asymmetries. *Journal of Econometrics*, **147**, 104–119.

Otranto, E. (2015). Adding flexibility to markov switching models. Technical report, CRENoS Working Paper 2015/09.

Whaley, R. E. (1993). Derivatives on market volatility: Hedging tools long overdue. *Journal of Derivatives*, **1**, 71–84.

Zadeh, L. (1965). Fuzzy sets. *Information and Control*, **8**, 338–353.

Tables and Figures

Table 1: Average values of the realized kernel volatility of S&P500 in correspondence of the regimes derived from MS(3)–AMEM and FR(2)–AMEM.

	Regime from MS(3)			Regime from FR(2)				
	1	2	3	1–crisp	1–fuzzy	2–fuzzy	2–crisp	total
average	9.22	17.23	35.06	7.60	16.10	13.25	47.51	13.86
frequency	1511	778	207	655	783	968	87	2496

Table 2: Estimation results (standard errors in parentheses) of a FR(3)–AMEM applied to four realized kernel volatilities of financial time series.

	ω	k_2	k_3	p_{11}	p_{12}	p_{21}	p_{22}	p_{31}	p_{32}
S&P500	1.25	1.58	10.56	0.68	0.13	0.01	0.99	1.00	0.00
	(0.19)	(0.21)	(2.77)	(0.04)	(0.04)	(0.00)	(0.00)	(0.01)	(0.00)
Russell 2000	1.52	1.78	2.75	0.78			0.99	0.95	0.05
	(0.21)	(0.16)	(0.53)	(0.05)			(0.00)	(0.02)	(0.02)
DJ 30	1.39	1.32	14.88	0.79	0.10	0.00	0.99	1.00	0.00
	(0.22)	(0.08)	(4.01)	(0.03)	(0.02)	(0.00)	(0.00)	(0.02)	(0.00)
Nasdaq 100	0.42	1.26	5.93	0.60	0.15	0.01	0.98	0.86	0.00
	(0.94)	(0.50)	(1.17)	(0.10)	(0.05)	(0.00)	(0.00)	(0.07)	(0.00)
	α_0	α_1	β_0	β_1	γ_0	γ_1	δ	c	a
S&P500	0.00	0.37	0.51	0.03	0.12	0.00	1.68	-0.28	16.72
	(0.00)	(0.03)	(0.04)	(0.00)	(0.01)	(0.00)	(0.12)	(0.05)	(0.66)
Russell 2000		0.39	0.49	0.03	0.07	0.06	1.15	-0.77	17.09
		(0.03)	(0.04)	(0.00)	(0.04)	(0.06)	(0.13)	(0.18)	(0.79)
DJ 30	0.00	0.35	0.52	0.03	0.08	0.04	1.57	-0.41	15.93
	(0.00)	(0.03)	(0.04)	(0.00)	(0.03)	(0.04)	(0.11)	(0.07)	(0.52)
Nasdaq 100	0.27	0.17	0.47	0.01	0.00	0.11	0.82	-0.09	21.29
	(0.07)	(0.10)	(0.05)	(0.01)	(0.01)	(0.03)	(0.22)	(0.59)	(1.11)

Table 3: Local average volatilities using alternative AMEM models for four US financial indices.

		S&P500	Russell 2000	DJ 30	Nasdaq 100
MS(3)	u_1	9.06	7.78	9.09	9.14
	u_2	14.28	11.91	14.37	14.77
	u_3	58.27	70.00	52.87	63.68
ST	u^l	5.86	10.28	5.77	7.97
	u^h	32.61	25.79	30.84	29.56
FR(2)	u_1^l	6.72	4.57	6.16	5.79
	u_1^h	40.69	41.36	33.13	39.10
	u_2^l	7.79	6.08	6.98	7.85
	u_2^h	41.76	42.86	33.95	41.16
FR(3)	u_1^l	2.88	3.15	3.18	1.61
	u_1^h	127.60	65.53	162.90	184.74
	u_2^l	4.46	4.93	4.50	2.87
	u_2^h	129.18	67.31	164.22	186.00
	u_3^l	15.01	7.68	19.38	8.80
	u_3^h	139.74	70.05	179.10	191.93

For the MS(3)–AMEM we show the LAV when $s_t = s_{t-1}$; for the ST–AMEM we show the lowest and highest theoretical LAV; for the FR(2)–AMEM and FR(3)–AMEM the lowest and highest theoretical volatility within each regime.

Table 4: Timetable of events corresponding to the Regime 2–crisp dates in model FR(2) for S&P500.

Dating	Related Events
17 Mar 2008	Collapse of Bear Stearns and contagion effect (Lehman shares fall as much as 48%)
17–18 Sep 2008	Aftermath of the Lehman Brothers collapse (15 Sep)
22 Sep-8 Dec 2008	Height of the financial crisis
6–7 May 2010	Flash crash (6 May)
18–19 May 2010	On May 18, Greece receives the first EUR 20 billion rescue package from EU and IMF
8–12 Aug 2011	Consequences of the Standard & Poor's downgrading of US credit rating from AAA to AA+ on 6 August 2011.
16 Aug 2011	Joint press conference Sarkozy–Merkel about European debt hinting at the possibility of Grexit.
18–30 Aug 2011	Contagion following market reactions to Euro debt crisis (on 18 Aug the European indices fall by 4.5-6%)

Table 5: Inference on the regime: number of indices with the volatility falling in the same regime at the same time, using three alternative models.

	Number of indices with the same state			
Model	Four	Three	Two pairs	Two
MS(3)–AMEM	43.09	45.37	10.41	1.12
FR(2)–AMEM	42.97	38.25	18.78	
FR(3)–AMEM	61.67	32.64	5.09	0.60

Table 6: P-values of the Ljung–Box statistics to test for autocorrelation at several lags: residuals and squared residuals from several models estimated on four US indices. The bold (resp. italics) numbers indicate no autocorrelation at 5% (resp. 1%) significance level.

	residuals				squared residuals			
	S&P500							
	LB(1)	LB(5)	LB(10)	LB(20)	LB(1)	LB(5)	LB(10)	LB(20)
HAR	0.009	0.000	0.000	0.000	0.000	0.000	0.000	0.000
AMEM	**0.227**	**0.486**	**0.153**	0.000	**0.585**	**0.604**	**0.172**	0.001
ST–AMEM	**0.457**	**0.515**	**0.056**	0.002	**0.339**	**0.495**	**0.061**	*0.011*
MS(3)–AMEM	**0.833**	**0.142**	**0.060**	0.001	**0.149**	*0.028*	0.009	0.000
FR(2)–AMEM	0.003	*0.020*	*0.045*	*0.022*	0.004	*0.034*	**0.078**	**0.057**
FR(3)–AMEM	**0.348**	**0.353**	*0.013*	0.000	**0.146**	**0.473**	*0.031*	0.006
	Russell 2000							
	LB(1)	LB(5)	LB(10)	LB(20)	LB(1)	LB(5)	LB(10)	LB(20)
HAR	*0.011*	0.000	0.000	0.000	0.000	0.000	0.000	0.000
AMEM	**0.140**	**0.227**	**0.052**	0.004	**0.551**	**0.211**	**0.228**	0.004
ST–AMEM	**0.759**	**0.548**	*0.043*	0.001	**0.558**	**0.268**	**0.199**	0.007
MS(3)–AMEM	0.000	0.000	0.000	0.000	0.000	0.000	0.000	0.000
FR(2)–AMEM	**0.063**	**0.236**	*0.028*	0.000	*0.036*	**0.234**	**0.107**	0.008
FR(3)–AMEM	**0.101**	**0.428**	*0.048*	0.001	**0.090**	**0.343**	**0.082**	0.006
	DJ 30							
	LB(1)	LB(5)	LB(10)	LB(20)	LB(1)	LB(5)	LB(10)	LB(20)
HAR	0.006	0.000	0.000	0.000	0.000	0.000	0.000	0.000
AMEM	**0.629**	**0.174**	**0.085**	0.002	**0.850**	**0.195**	*0.047*	*0.034*
ST–AMEM	**0.179**	**0.117**	*0.026*	*0.014*	**0.134**	**0.092**	*0.036*	**0.127**
MS(3)–AMEM	**0.165**	0.003	*0.013*	**0.050**	*0.014*	0.001	0.003	*0.027*
FR(2)–AMEM	0.002	0.003	0.006	*0.016*	0.005	0.005	*0.015*	**0.077**
FR(3)–AMEM	*0.035*	*0.034*	0.002	0.001	*0.025*	**0.088**	*0.018*	**0.070**
	Nasdaq 100							
	LB(1)	LB(5)	LB(10)	LB(20)	LB(1)	LB(5)	LB(10)	LB(20)
HAR	*0.025*	0.000	0.000	0.000	0.000	0.000	0.000	0.000
AMEM	*0.010*	0.003	0.000	0.000	**0.119**	**0.128**	*0.021*	0.000
ST–AMEM	**0.447**	*0.018*	0.000	0.000	**0.984**	**0.324**	**0.065**	*0.011*
MS(3)–AMEM	*0.030*	0.000	0.000	0.000	**0.482**	*0.030*	0.000	0.000
FR(2)–AMEM	*0.020*	0.000	0.000	0.000	0.007	0.003	0.009	*0.022*
FR(3)–AMEM	**0.868**	0.006	0.004	0.000	**0.481**	**0.077**	**0.079**	*0.037*

Table 7: In–sample and 1-step and 10-steps out–of–sample performance of several models for four US indices, calculated in terms of MSE and MAE. The bold numbers indicate the best performance, the italic numbers the second best.

	In–Sample		Out–of–Sample			
	S&P500					
	MSE	MAE	MSE 1	MAE 1	MSE 10	MAE 10
HAR	27.563	3.102	7.564	2.131	111.530	7.928
AMEM	25.925	2.989	7.048	2.072	119.236	9.228
ST–AMEM	24.567	2.935	*6.720*	*2.044*	**83.002**	**7.010**
MS(3)–AMEM	*19.926*	**2.615**	7.644	2.134	104.646	7.967
FR(2)–AMEM	23.277	2.773	**6.606**	**2.018**	91.004	*7.212*
FR(3)–AMEM	**19.419**	*2.654*	6.933	2.079	*89.012*	7.364
	Russell 2000					
	MSE	MAE	MSE 1	MAE 1	MSE 10	MAE 10
HAR	28.008	3.333	8.176	2.280	90.730	*7.324*
AMEM	26.147	3.242	8.654	2.370	117.202	9.278
ST–AMEM	25.234	3.220	7.775	2.234	*84.656*	7.628
MS(3)–AMEM	**19.537**	**2.776**	8.274	2.243	**77.379**	**6.650**
FR(2)–AMEM	23.880	3.114	*7.537*	*2.174*	100.098	7.911
FR(3)–AMEM	*22.666*	*2.903*	**7.485**	**2.168**	85.728	7.413
	DJ 30					
	MSE	MAE	MSE 1	MAE 1	MSE 10	MAE 10
HAR	28.063	3.096	9.072	2.262	108.601	7.875
AMEM	26.557	2.983	8.068	2.143	108.320	8.665
ST–AMEM	25.490	2.930	*7.776*	*2.087*	**79.895**	**7.053**
MS(3)–AMEM	*20.501*	**2.661**	8.987	2.224	103.634	7.984
FR(2)–AMEM	24.450	2.828	**7.724**	**2.044**	98.820	7.542
FR(3)–AMEM	**20.071**	*2.735*	7.941	2.115	*85.271*	*7.311*
	Nasdaq 100					
	MSE	MAE	MSE 1	MAE 1	MSE 10	MAE 10
HAR	18.523	2.545	7.198	2.152	101.635	7.982
AMEM	18.119	2.519	7.979	2.353	102.225	8.582
ST–AMEM	17.159	2.477	*6.423*	*2.030*	**79.577**	**7.147**
MS(3)–AMEM	**12.072**	**2.114**	7.054	2.127	92.999	7.637
FR(2)–AMEM	15.949	2.316	**6.266**	**1.973**	105.288	7.927
FR(3)–AMEM	*13.651*	*2.212*	6.547	2.055	*83.303*	*7.450*

Table 8: Global Loss functions of several models for four US indices. The bold numbers indicate the best performance, the italic numbers the second best.

	S&P500			
	uniform	oos oriented	oos st oriented	oos lt oriented
HAR	0.000	0.000	0.000	0.000
AMEM	0.007	0.018	-0.015	0.051
ST–AMEM	-0.114	**-0.121**	-0.099	**-0.143**
MS(3)–AMEM	-0.080	-0.052	-0.046	-0.059
FR(2)–AMEM	*-0.119*	-0.117	**-0.107**	-0.126
FR(3)–AMEM	**-0.137**	*-0.120*	*-0.104*	*-0.137*
	Russell 2000			
	uniform	oos oriented	oos st oriented	oos lt oriented
HAR	0.000	0.000	0.000	0.000
AMEM	0.094	0.122	0.076	0.168
ST–AMEM	-0.038	-0.032	-0.037	-0.028
MS(3)–AMEM	**-0.119**	**-0.096**	*-0.072*	**-0.119**
FR(2)–AMEM	-0.026	-0.010	-0.040	0.021
FR(3)–AMEM	*-0.083*	*-0.067*	**-0.076**	*-0.058*
	DJ 30			
	uniform	oos oriented	oos st oriented	oos lt oriented
HAR	0.000	0.000	0.000	0.000
AMEM	-0.026	-0.022	-0.048	0.004
ST–AMEM	*-0.122*	*-0.132*	*-0.117*	**-0.147**
MS(3)–AMEM	-0.078	-0.053	-0.052	-0.053
FR(2)–AMEM	-0.099	-0.097	-0.108	-0.086
FR(3)–AMEM	**-0.146**	**-0.135**	**-0.126**	*-0.145*
	Nasdaq 100			
	uniform	oos oriented	oos st oriented	oos lt oriented
HAR	0.000	0.000	0.000	0.000
AMEM	0.042	0.053	0.065	0.041
ST–AMEM	-0.098	*-0.107*	*-0.092*	*-0.123*
MS(3)–AMEM	*-0.113*	-0.084	-0.074	-0.093
FR(2)–AMEM	-0.069	-0.060	-0.084	-0.035
FR(3)–AMEM	**-0.129**	**-0.116**	**-0.105**	**-0.127**

Figure 1: Theoretical behavior of the LAV in regime 1 (lower curve) and regime 2 (upper curve) in correspondence of the smooth transition function g_t. The gray area represents the fuzzy zone. Parameter values: $\omega = 1$, $k_2 = 3$, $\alpha_0 = 0.5$, $\alpha_1 = 0.4$, $\beta_0 = 0$, $\beta_1 = 0$, $\gamma_0 = 0$, $\gamma_1 = 0$.

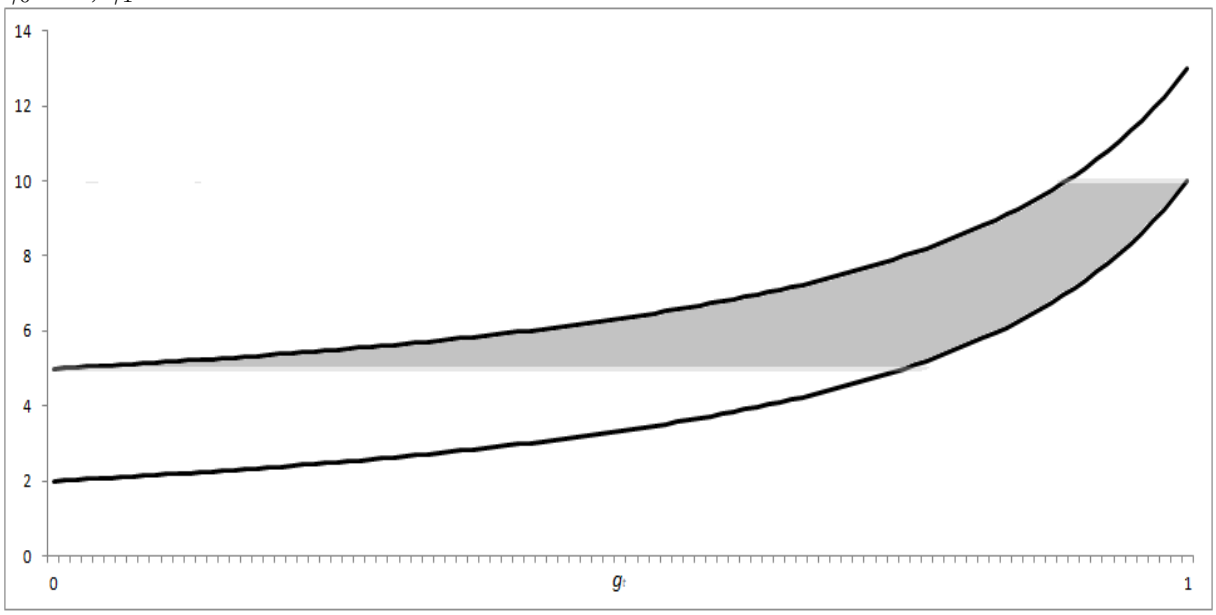

Figure 2: Realized kernel volatility of four US market indices. The dates on the x-axis are in correspondence of the beginning of the year.

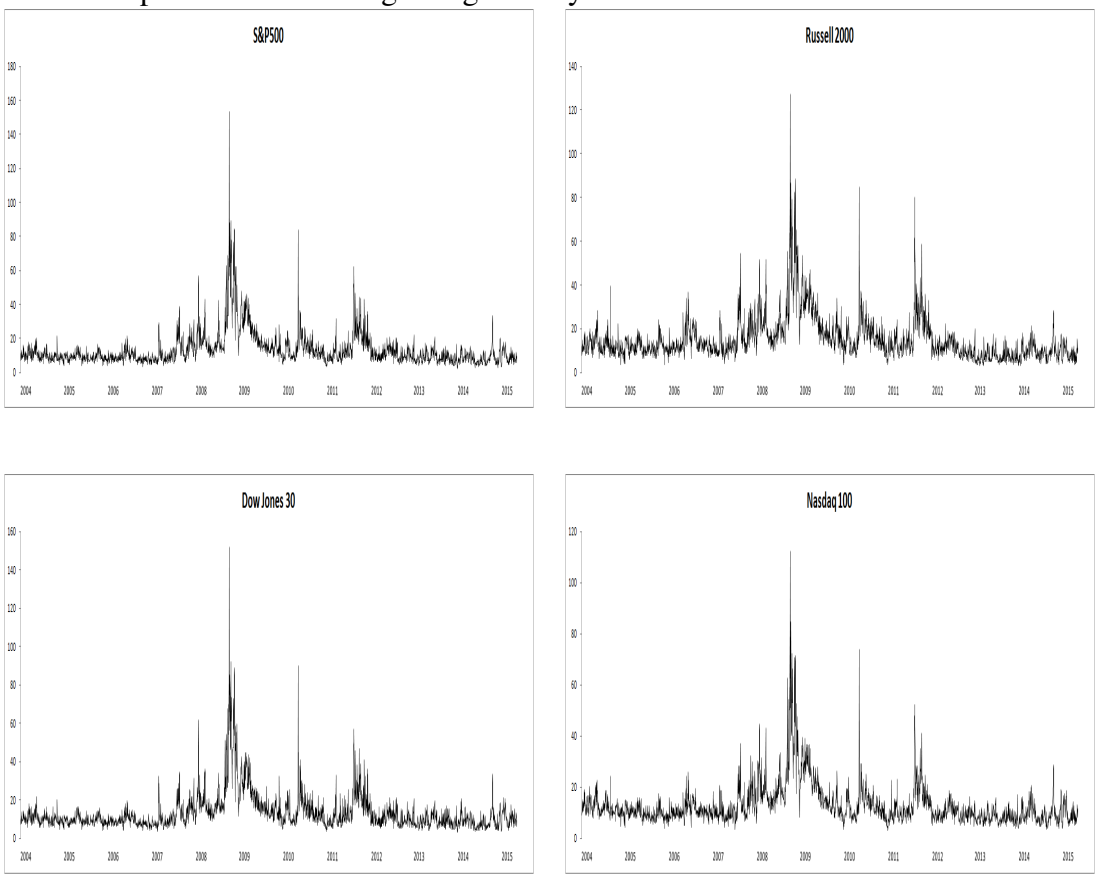

Figure 3: S&P500 index: realized kernel volatility (black line) and LAV (blue line) derived from three alternative models. The dates on the x-axis are in correspondence of the beginning of the year.

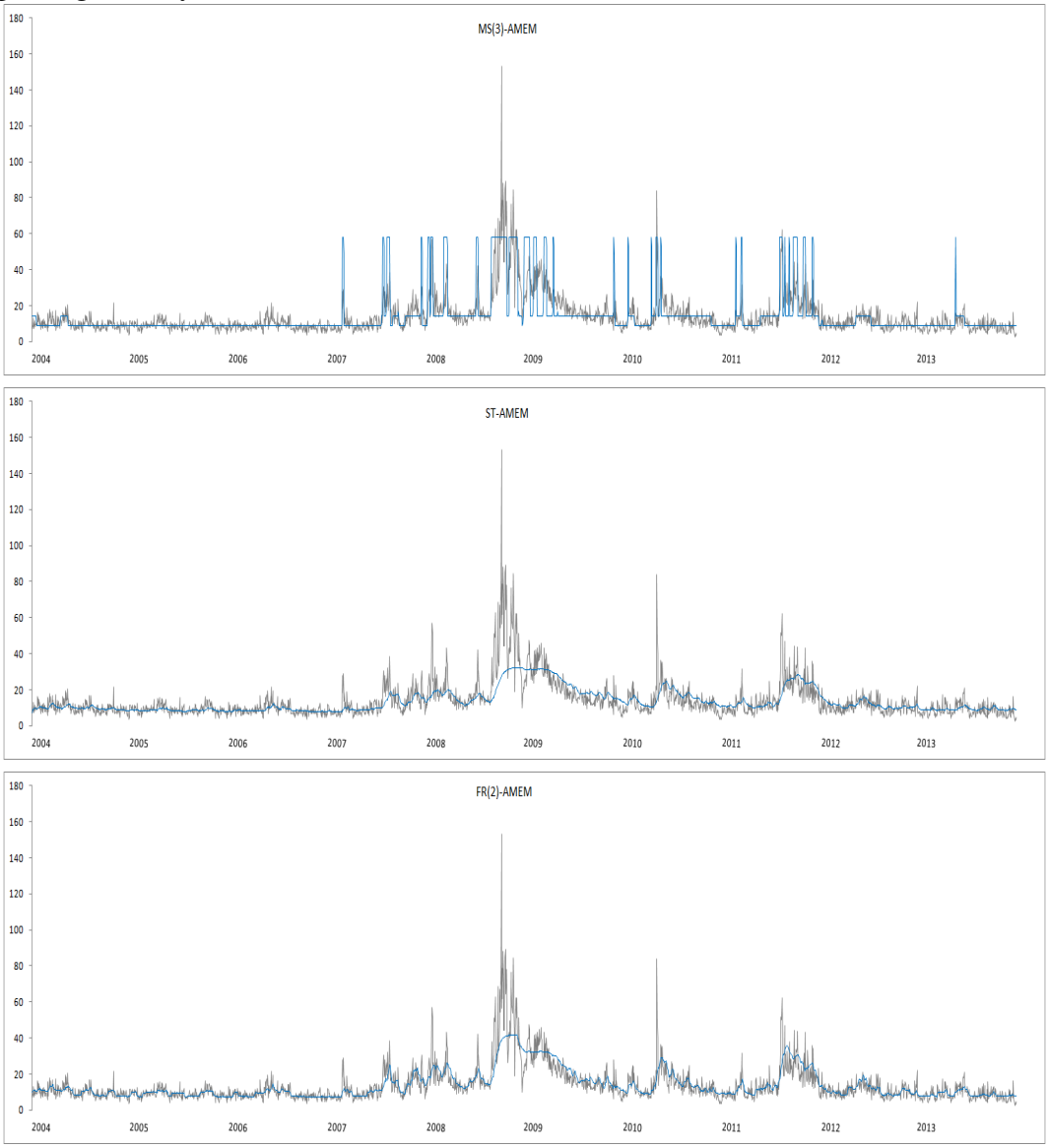

Figure 4: S&P500 index: Distribution of the realized volatility in terms of regimes derived from the MS(3)–AMEM and the FR(2)–AMEM.

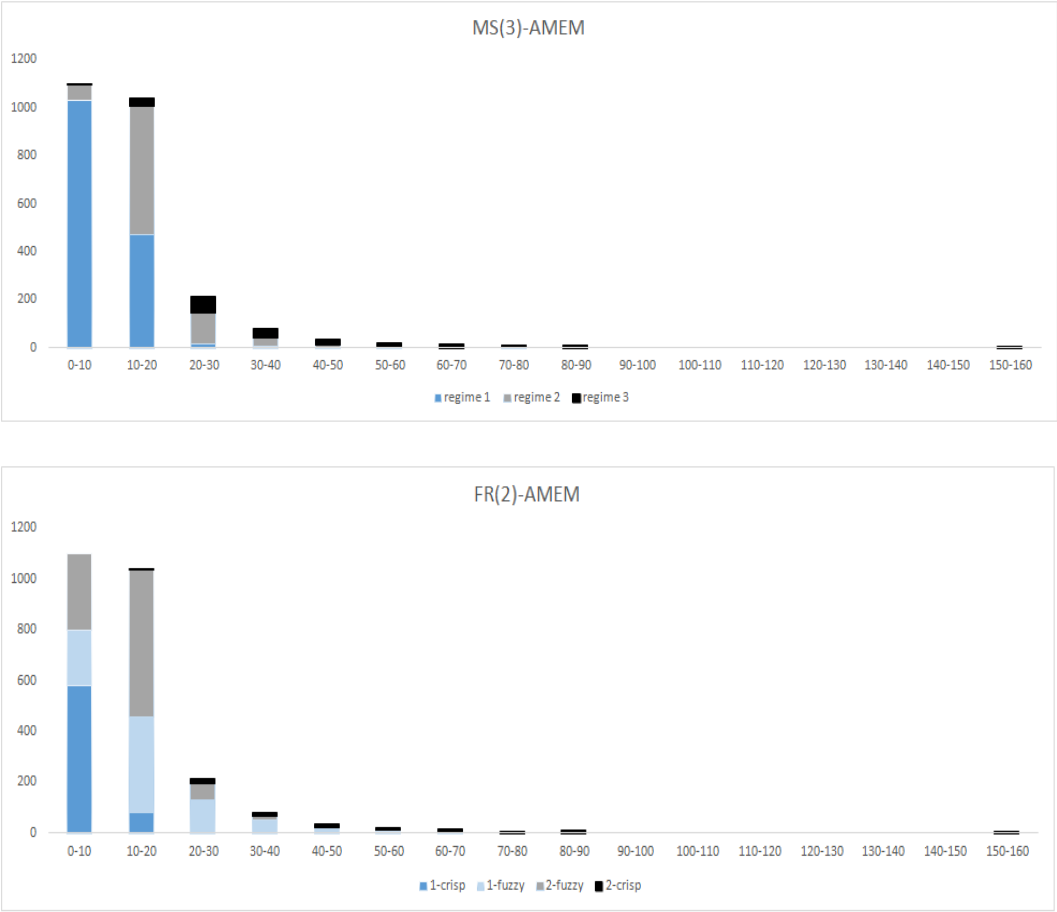

Figure 5: S&P500 index: realized kernel volatility and inference on the regime (right axis), distinguishing fuzzy regimes (blue dotted line) and crisp regimes (black continuous line); the results are derived from a FR(2)–AMEM. The dates on the x-axis are in correspondence of the beginning of the year.